Transition from quasiperiodicity to chaos in a Josephson-junction analog

Da-Ren He, W. J. Yeh, and Y. H. Kao
Department of Physics, State University of New York at Stony Brook, Stony Brook, New York 11794
(Received 18 November 1983)

Experimental observations of the transition from quasiperiodicity to chaos are carried out with an electronic Josephson-junction simulator driven by two independent ac sources. A Poincaré section shows an invariant ellipse when the frequency ratio of the two input currents is very close to the reciprocal of the golden mean. The system enters a chaotic state at high input-current amplitudes characterized by a breakdown of the smooth ellipse at the onset of transition. Two convergence ratios are experimentally determined, showing good agreement with calculated values obtained by circle map studies.

I. INTRODUCTION

The transition to chaos in dynamical systems has been a subject of many theoretical and experimental studies in recent years.[1] Results have shown that there may be several distinct routes to chaos in a system, depending on the manner and range in which some characteristic parameters are varied. Considerable progress has been made, in particular, on routes to chaotic behavior via period-doubling bifurcation[2] and intermittency.[3] Of special interest in these cases are the predictions by renormalization-group analyses and experimental observations of universality and scaling behavior at the onset of chaos, independent of the details of the physical systems under investigation. More recently, another route to chaos, namely through quasiperiodic behavior with two incommensurate frequencies, has been studied by several theory groups, and some universal properties associated with such a transition have also been suggested.[4] Yet no comparison has been made between experimental data pertaining to this type of transition and the theoretically predicted behavior.

In this paper we present results of direct experimental observations of the transition from quasiperiodicity to chaos by using a Josephson-junction (or damped pendulum) simulator. The Poincaré section observed in this measurement lends support to the existence of an invariant circle characterized by an approximated irrational winding number, and the emergence of chaos is signified by the destruction of a smooth invariant circle. Two convergence ratios determined in our experiment are in good agreement with the values obtained by circle-map studies.[4]

II. QUASIPERIODICITY IN A JOSEPHSON-JUNCTION SIMULATOR

The Josephson-junction system is well known for its rich content of nonlinear dynamical behavior. The transition to chaos through period-doubling bifurcation and intermittency routes in this system has been studied by numerical solutions[5] of the equation of motion and by direct physical measurements of an electronic junction simulator.[6] In our previous measurements of this simulator driven by an external ac source,[6] universal scaling behavior near the onset of transition has been observed, from which several critical exponents are experimentally determined. It is natural to anticipate that if the simulator were driven by two ac sources with incommensurate frequencies, a new type of transition from quasiperiodicity to chaos should occur; this is borne out in our experiments.

The simulator used in the present experiment is the same as the one we used before,[6] making use of a circuit designed by Magerlein.[7] The actual circuit including the external sources is shown in Fig. 1. In this figure, J is the Josephson-junction simulator, C is a capacitor, and R_S is a shunt resistor. The current in J is proportional to $\sin\phi$, and the instantaneous voltage across its terminals $v_{ab}(t)$ is proportional to the time derivative of ϕ, thus ϕ plays the same role as the quantum phase difference between the two superconductors in a Josephson tunnel junction. The shunt resistance R_S represents the channel of quasiparticle current flow in the junction, hence the system is inherently dissipative. The parallel combination of J, C, and R_S thus simulates the essential dynamical behavior of a Josephson tunnel junction. The ac voltmeter V measures the rms value of v_{ab}, and either an oscilloscope or a power-spectrum analyzer can be connected to the terminals ab when needed, in order to measure the time varia-

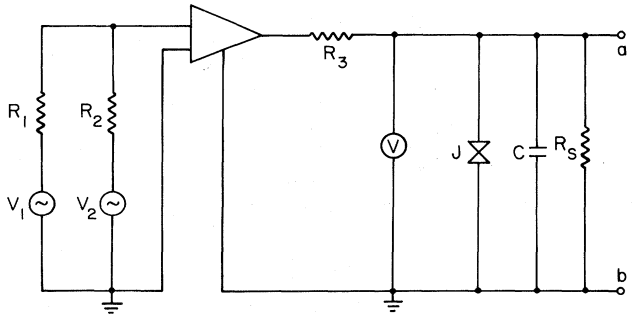

FIG. 1. Circuit used in the present experiment for studying quasiperiodicity and chaos. $R_1=R_2=40.7$ kΩ and $R_3=50$ Ω. V is an ac voltmeter. J is the Josephson-junction simulator. $C=0.07$ μF, $R_s=1$ kΩ, and $\omega_0=28.7$ kHz.

tion of v_{ab} or its power spectral density. The ac voltage sources V_1 and V_2, together with the series resistors R_1 and R_2, form two current sources with separately tunable frequencies. The time dependence of $\phi(t)$ is governed by the following differential equation due to current conservation:

$$\frac{d^2\phi}{dt^2}+\frac{1}{(\beta_c)^{1/2}}\frac{d\phi}{dt}+\sin\phi=A_1\sin\omega_1 t+A_2\sin(\omega_2 t+\gamma)\ , \tag{1}$$

where $\beta_c=2eI_cR^2C/\hbar$ is the McCumber parameter,[8] the amplitudes A_1, A_2 of the applied ac currents are normalized to the junction's critical current I_c, the angular frequencies ω_1, ω_2 are normalized to the plasma frequency $\omega_0=(2eI_0/\hbar C)^{1/2}$, the time t is normalized to $1/\omega_0$, and γ is a phase constant.

There are certain advantages in studying the junction simulator, as opposed to the actual Josephson junctions. First, the oscillation frequency of ϕ can be set at a rather low value so that the time variation of $d\phi/dt$ and its power spectrum can be easily measured with conventional instruments. Second, the supercurrent term $\sin\phi$ can be directly monitored, allowing detailed measurements of its time dependence to be made. Third, the power output across the junction terminals can be adjusted to a relatively high level which is convenient to direct power-spectrum observations. In the context that a real current-driven Josephson junction is also described essentially by Eq. (1), the simulator actually permits more physical studies to be made with greater versatility than a real junction.

III. RESULTS AND DISCUSSION

As can be seen from the studies of chaos in the past, theoretical predictions are usually based on analyses of some special maps, while experimental observations are often made with systems more conveniently described by differential equations. Under most circumstances, although the scaling behavior might be independent of the mechanisms pursued, a direct unequivocal identification of physical observables between theory and experiment is rather difficult. This situation is more of a problem in the present case because no quantitative guidelines are available as to how a Josephson junction driven by two ac sources at incommensurate frequencies will enter chaos. We therefore take the standpoint that no attempt will be made for the purpose of verifying any theoretical predictions on the transition from quasiperiodicity to chaos. Comparisons between our physical observations and the theoretical results will only be tried, however, on a semiquantitative basis in cases where such a comparison might serve an indicative purpose. We also hope this work will stimulate more theoretical interest in studying the transition to chaos by means of differential equations.

A. Poincaré sections and power spectra

In all the results shown below, the following parameter values have been used: $R_S\cong 1.0$ kΩ, $C\cong 0.07$ μF, $I_c\cong 1.04$ mA, $\omega_0\cong 28.7$ kHz, and $\beta_c\cong 4$. In accordance

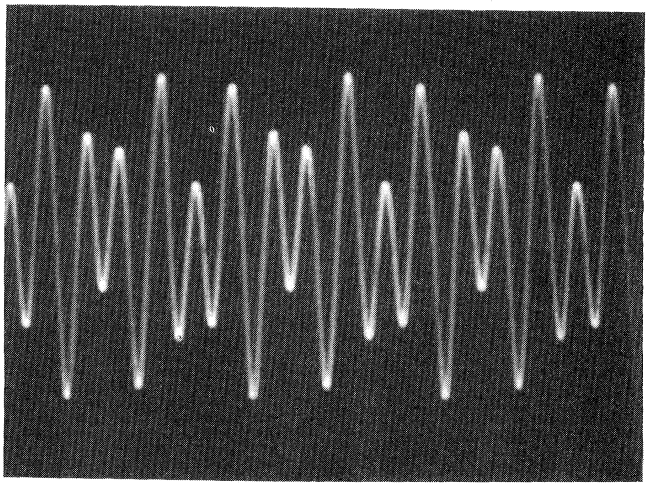

(a)

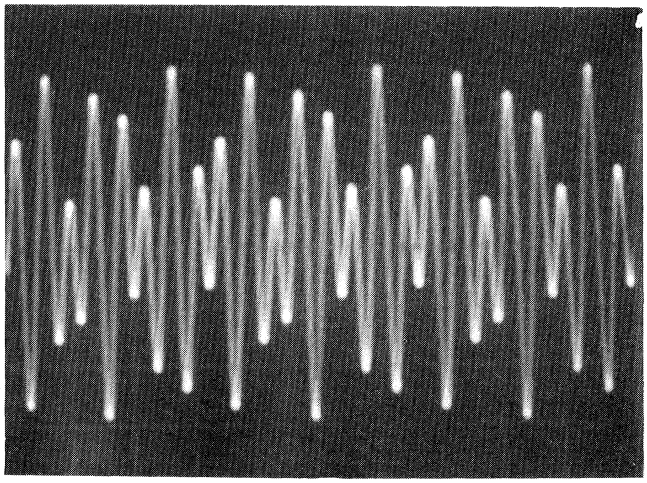

(b)

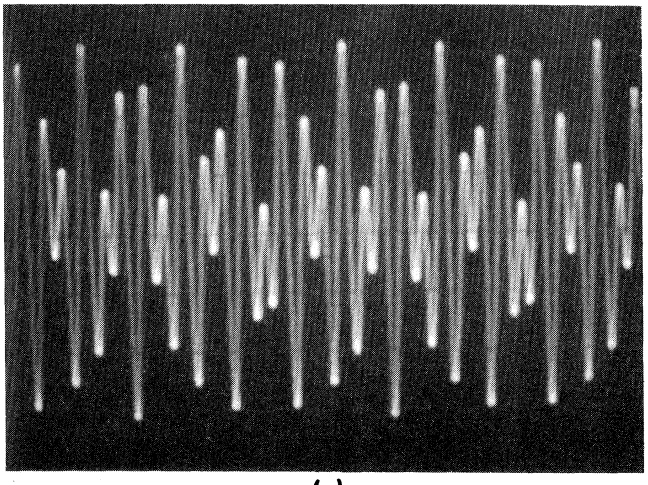

(c)

FIG. 2. Oscilloscope traces of $\dot{\phi}(t)$ vs t. (a) $\omega_1\cong 0.65$, $\omega_2=1.09$, $W=\frac{3}{5}$, $A_1/A_{1c}=0.192$, and $A_2/A_{2c}=0.096$. (b) $\omega_1\cong 0.68$, $\omega_2=1.09$, $W=\frac{5}{8}$, $A_1/A_{1c}=0.143$, and $A_2/A_{2c}=0.101$. (c) $\omega_1\cong 0.67$, $\omega_2=1.09$, $W=\frac{8}{13}$, $A_1/A_{1c}=0.252$, and $A_2/A_{2c}=0.101$.

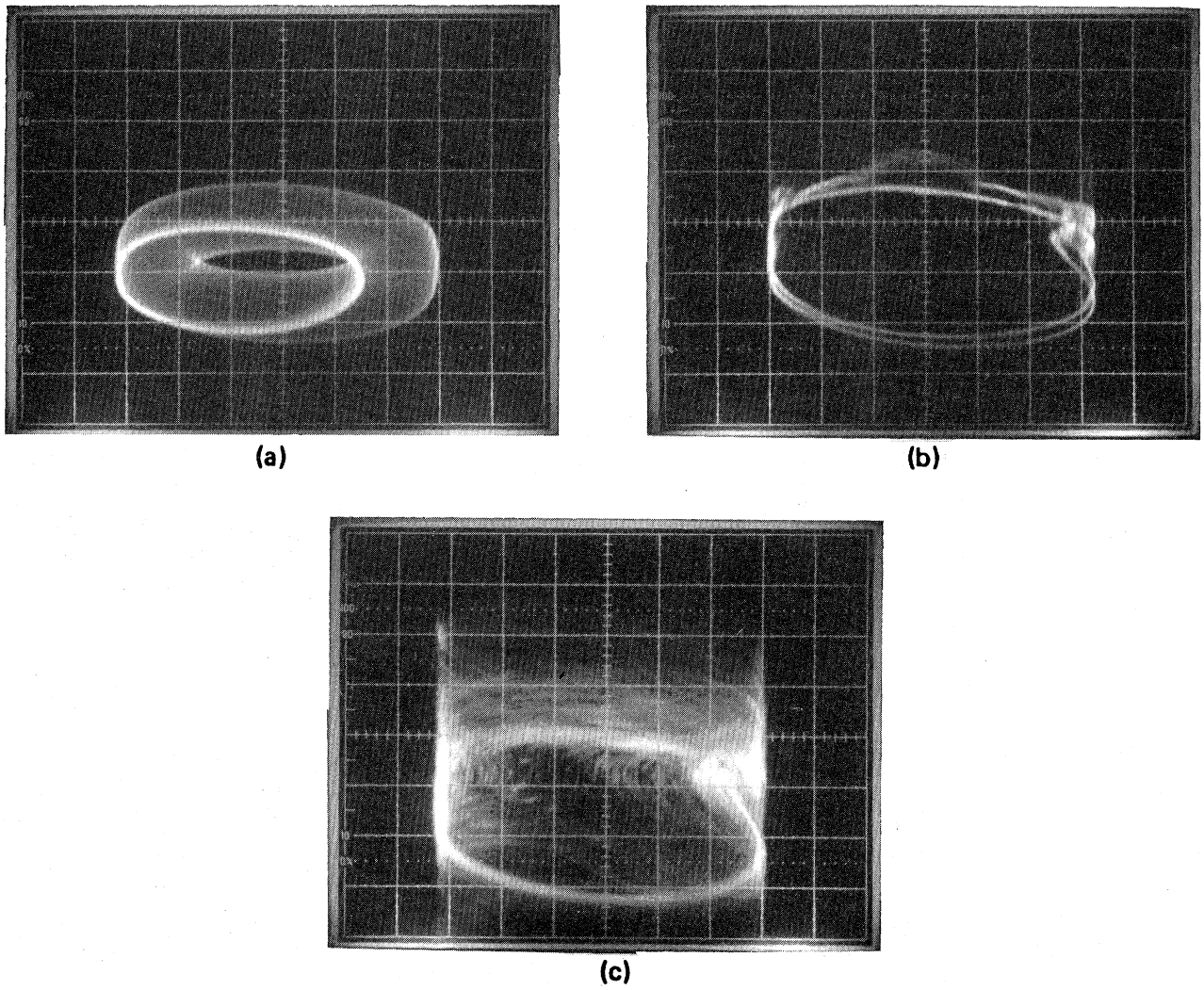

FIG. 3. Sequence of Poincaré sections from quasiperiodicity to chaos obtained by plotting $\sin\phi$ against $\dot{\phi}$; $\omega_1=0.4059$, $\omega_2=0.6568$, $\omega_1/\omega_2\cong\overline{W}$. (a) The bright ellipse is obtained with a discrete time interval (z axis triggering the oscilloscope beam at a frequency equal to that of V_2, 3.0 kHz). $A_1=0.5224$ and $A_2=0.1600$. The torus is the same plot of $\sin\phi$ vs $\dot{\phi}$ with the same parameters except that free running time is used (internal triggering instead of z-axis triggering.) (b) Onset of chaos characterized by the appearance of kinks. $A_1=0.7651$ and $A_2=0.1608$. (c) Chaotic regime. $A_1=0.7656$ and $A_2=0.1608$.

with our previous work on chaos in this system,[6] the reduced angular frequencies ω_1 and ω_2 are usually chosen in the range 0.4–0.7, where the simulated junction system has a rich content of chaotic behavior. To examine the time variation of this system, we have chosen $\dot{\phi}$ $(=d\phi/dt)$ as the physical variable for observations of transition to chaos. Some typical traces of $\dot{\phi}$ versus t are shown in Fig. 2. In these curves, the frequency ratio ω_1/ω_2 has been specifically chosen to be $\frac{3}{5}$, $\frac{5}{8}$, $\frac{8}{13}$, respectively, as can be seen from the well-defined periodicity in each trace.

The variation of $\dot{\phi}$ can also be observed at discrete time intervals on an oscilloscope by triggering the beam at a frequency equal to that of V_2 and displaying $\dot{\phi}$ on the x axis. This allows us to map out a Poincaré section. To aid the eyes in observing the changes in the system as a two-dimensional pattern, we have somewhat arbitrarily chosen $\sin\phi$ as a generalized variable displayed on the y axis. Thus, by triggering the oscillosope at the frequency of V_2, a set of Q points will be shown on the screen if the ratio ω_1/ω_2 is equal to a rational winding number $W=P/Q$, with P and Q being relatively prime integers. This set of discrete points represents a Poincaré section (in the $\sin\phi$–$\dot{\phi}$ plane), which can be used to characterize the transition to chaos.

If the winding number W is chosen to approximate an irrational number, for instance, the reciprocal of the golden mean $\overline{W}=\frac{1}{2}(\sqrt{5}-1)$, this would correspond to a "smearing" of the Q-cycle points described above, and a continuous curve appears. For the parameters we used, this continuous curve on the $\sin\phi$–$\dot{\phi}$ plane usually takes the shape of an ellipse for low input-current amplitudes A_1 and A_2. Such a continuous curve obtained with $\omega_1/\omega_2\cong\overline{W}$ is shown in Fig. 3(a). For the sake of comparison, we also display a plot of $\sin\phi$ versus $\dot{\phi}$ in the same figure, but with a free-running-time variable, the resulting

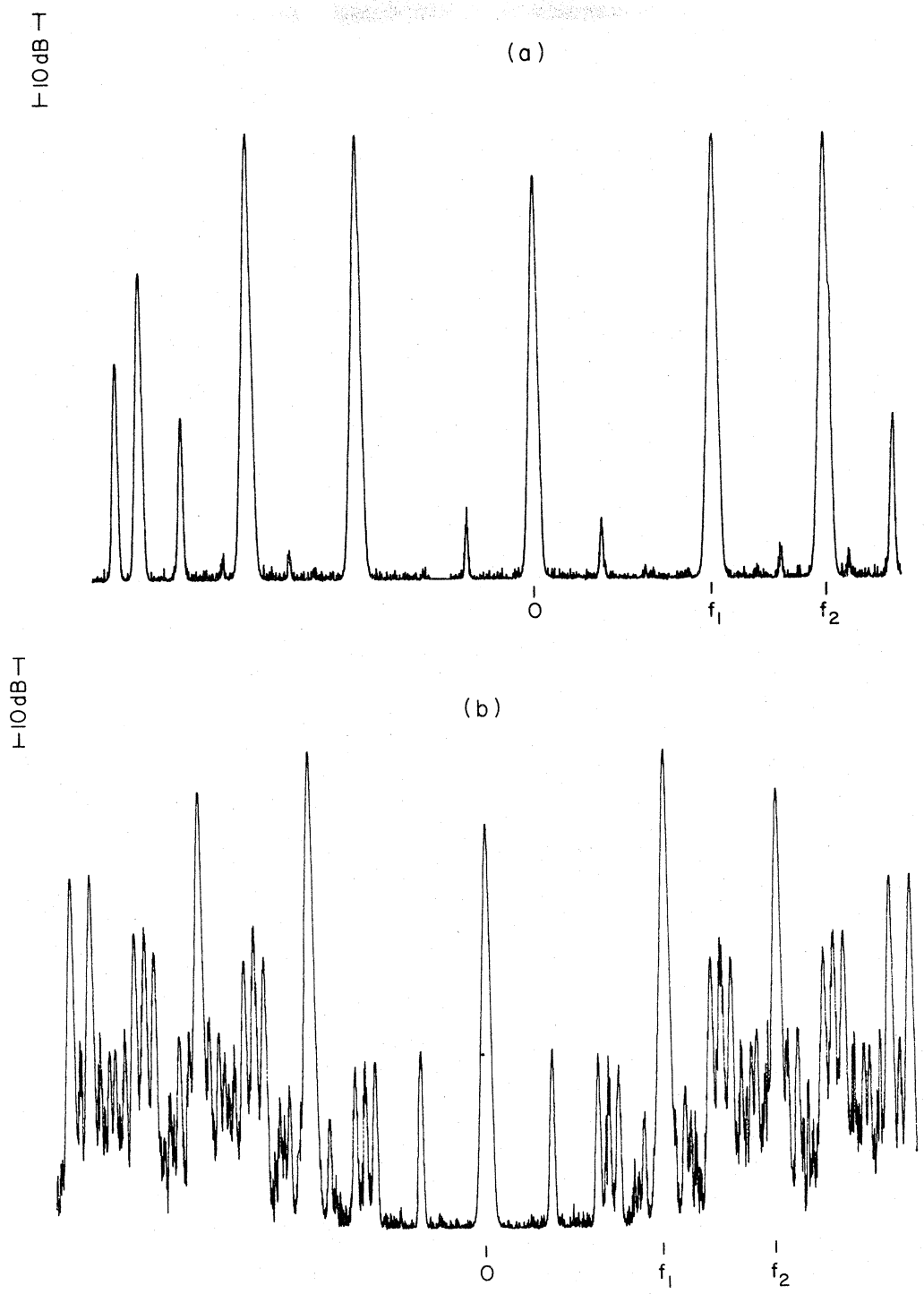

FIG. 4. Sequence of power spectra density curves from quasiperiodicity to chaos. (a) Quasiperiodic regime, (b) onset of chaos, and (c) chaotic regime, with parameters same as those for Figs. 3(a), 3(b), 3(c), respectively. $f_1=1.854$ kHz, $f_2=3.000$ kHz, and the peak at $f=0$ is an instrument marker. The frequency scale is linear.

curve is a two-dimensional torus. Note that although our choice of $\sin\phi$ as the ordinate is arbitrary, it is interesting to see that by using the two time-dependent functions $\sin\phi$ and $\dot{\phi}$ as generalized variables, the stationary curve in the $\sin\phi$—$\dot{\phi}$ space has a smooth invariant closed form at low values of A_1 and A_2. This plot of $\sin\phi$ versus $\dot{\phi}$ also shows the relationship between the supercurrent and the quasiparticle current in a Josephson junction. In a broad sense, this ellipse may be considered as a representation of an invariant circle associated with an irrational winding number.

If the amplitude of V_1 is increased to higher values

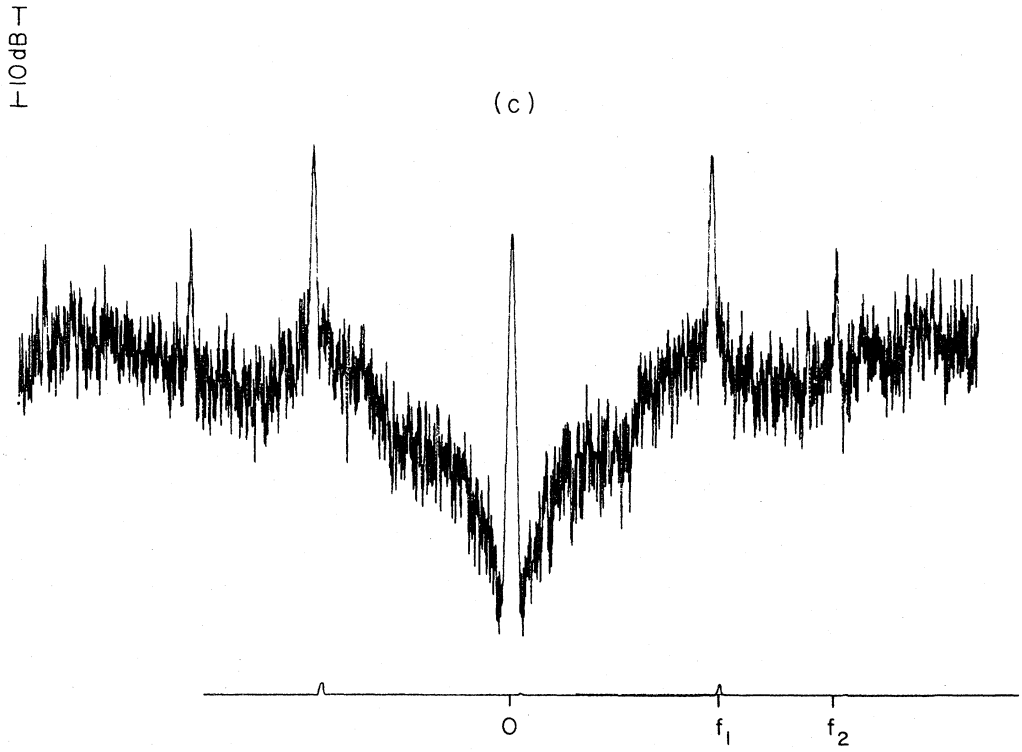

FIG. 4. (*Continued.*)

while keeping the frequencies unchanged, with ω_1/ω_2 approximately equal to $\overline{W}$, the system may exhibit a transition from quasiperiodicity to chaos. We define the chaotic region by the appearance of high broadband noise in the power spectrum of $\dot{\phi}$. It is significant to compare the main features appearing in the changes of the power spectrum with those of the Poincaré section described above. A sequence of the corresponding curves obtained by two different measurements but with the same parameters is shown in Figs. 3 and 4.

In Fig. 3(a), A_1 and A_2 are at low values, its corresponding power spectrum [Fig. 4(a)] has a simple form, showing mainly the components of the two driving frequencies and some beats. When A_1 is increased to a higher value, as shown in Fig. 4(b), the power spectrum shows a larger number of beats and an increased broadband noise; this condition is defined as the onset of chaos. A slight increase in A_1 beyond this point gives rise to a much higher noise and chaotic spectrum, except for the main peaks due to the driving frequencies [Fig. 4(c)]. The Poincaré section corresponding to the onset of chaos is shown in Fig. 3(b). A most interesting feature is the destruction of the smooth stationary elliptic curve observed before. There are conspicuous distortions in the otherwise smooth ellipse, which can be generally called "kinks." It appears that the existence of a kink is *always* associated with the onset of chaos, hence it can be viewed as a signature of the transition to chaotic behavior from quasiperiodicity. Under most conditions we have found that the kinks appear on a single ellipse, but occasionally the ellipse "splits" at the onset of chaos, as shown in Fig. 3(b); this may suggest the possibility of a bifurcation prior to chaos.[9] The Poincaré section corresponding to chaos [Fig. 4(c)] is shown in Fig. 3(c), where the stationary curve is almost completely distorted and turns into an open quasirandom curve, nearly filling in the available phase space. This sequence of curves clearly demonstrates the transition from quasiperiodicity to chaos.

The parameters which control the nonlinearity in the quasiperiodic region are the current amplitudes A_1 and A_2, with ω_1/ω_2 set at approximately $\overline{W}$. We define A_{1c} as the critical amplitude of A_1 at the onset of chaos when A_2 is set equal to 0 while keeping the frequencies unchanged. Likewise, A_{2c} is defined when A_1 is set equal to 0. There can be different combinations of the A_1 and A_2 values giving rise to an onset of transition from quasiperiodicity to chaos. Hence, in the A_1-A_2 space the chaotic and quasiperiodic domains are separated by a curve. This situation is in contrast to that of the one-dimensional map on a circle,

$$f(\theta)=\theta+\Omega-\frac{K}{2\pi}\sin 2\pi\theta\ , \tag{2}$$

where nonlinearity is characterized by a single parameter K, and the two "domains" are separated by a point at $K=K_c$.

The curve separating the chaotic and quasiperiodic domains in the A_1-A_2 space obtained with $\omega_1/\omega_2\cong\overline{W}$ is shown in Fig. 5. The two different regions may be considered as two distinct phases of the system. In a broad sense, when the system changes from one region to the other, it may be viewed as a phase transition. In the chaotic region above the phase-separation curve of this figure, some "window" regions can exist (not shown in the figure) where the system is quasiperiodic. These windows often occur near the edges where $A_1\gtrsim 0$ or $A_2\gtrsim 0$. In our

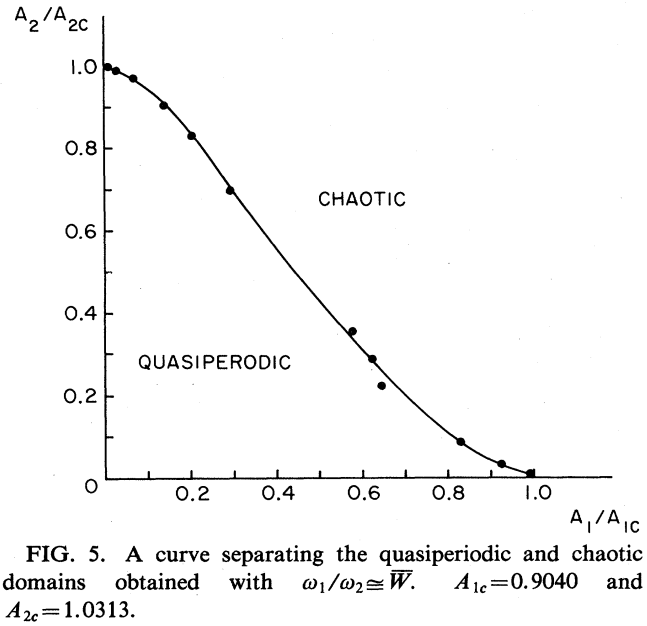

FIG. 5. A curve separating the quasiperiodic and chaotic domains obtained with $\omega_1/\omega_2 \cong \overline{W}$. $A_{1c}=0.9040$ and $A_{2c}=1.0313$.

observations, however, no window has been found experimentally in the middle region above the phase-separation curve.

B. Scaling behavior and convergence ratios

It would be interesting to find a physical quantity which is directly related to the winding number as well as the nonlinearity parameters, and yet permits us to examine its scaling behavior. To this end, we have measured the rms value of the ac voltage $\dot{\phi}(t)$ with an ac voltmeter for various sets of the driving-current amplitudes and frequencies. This rms value, denoted by $\overline{V}$, may be regarded as a quantity equivalent to the parameter Ω in the circle map given in Eq. (2).

Theoretical studies[4] have shown that

$$\Omega_n - \Omega_\infty \cong \delta^{-n} \tag{3a}$$

and

$$f^{F_n}(0) - F_{n-1} \cong \alpha^{-n} , \tag{3b}$$

where Ω_n is the value of Ω such that there is a cycle with winding number $W_n = F_n/F_{n+1}$ passing through $\theta=0$, and F_n is the nth Fibonacci number ($F_0=0, F_1=1, F_{n+1}=F_n+F_{n-1}$). For $|K|<1$, α and δ should take on the following values:

$$\delta = -\overline{W}^{-2} = -2.618\,033\,9\ldots , \tag{4a}$$

$$\alpha = -\overline{W}^{-1} = -1.618\,033\,9\ldots . \tag{4b}$$

Owing to inherent noise problems in the electronic circuit and limited instrument precision, we could only measure $\overline{V}$ values with the winding number W_n up to $n=6$, i.e., $W_6=\frac{8}{13}$. Using Eq. (3a), similar to the definitions given in Ref. 4, we define a convergence ratio δ_n as

$$\delta_n = \frac{\overline{V}_{n-1} - \overline{V}_{n-2}}{\overline{V}_n - \overline{V}_{n-1}} , \tag{5}$$

where $\overline{V}_n$ is the value of $\overline{V}$ corresponding to the winding number $W_n = F_n/F_{n+1}$. From the measured values of $\overline{V}_4$, $\overline{V}_5$, and $\overline{V}_6$ obtained with different sets of A_1 and A_2, we have computed δ_6 and obtained an average,

$$\delta_6 = -2.75 \pm 0.2 . \tag{6}$$

It can be seen that although only up to $n=6$ in the $\overline{V}_n$ sequence is obtainable in our experiment, the measured convergence ratio δ_6 is in reasonably good agreement with the calculated δ value for $|K|<1$ in the circle map.[4]

Likewise, we have also determined the constant α from our data. We let d_n denote the value of the element on the F_{n+1} cycle closest to $\theta=0$ in the circle map (modulo 1) with winding number $W_n = F_n/F_{n+1}$; it follows from Eq. (3b) that a convergence ratio α_n can be defined as $\alpha_n(K) = d_{n-1}/d_n$. In order to find d_n in our measurements, we have made use of the $\dot{\phi}$ versus t plots similar to those shown in Fig. 2. For a given set of A_1, A_2 and a winding number, say $W_6=\frac{8}{13}$, we have 13 nonrepetitive peaks in a $\dot{\phi}(t)$ plot; the instantaneous voltages at these peaks are recorded and then arranged in the order of progressively increasing values. This sequence of monotonically increasing $\dot{\phi}$ peak values may be assumed as a one-to-one correspondence with a sequence of points on a circle map. This is not inconsistent with the recent work by Jensen, Bohr, Christiansen, and Bak,[10] in which it was shown that the return map of $\dot{\phi}$ in Eq. (1) is a circle map.

In view of the fact that $\dot{\phi}(t)$ is bounded and periodic in this region (A_1 and A_2 are below the onset of chaos and with a rational winding number $W_n = F_n/F_{n+1}$ when n is not large), we conjecture that $\dot{\phi}(t)$ plays the role of $\theta_{n+1} - \theta_n$ in the circle map. For simplicity, we assume $\dot{\phi} = r\cos(\theta - \theta_0)$. With this assignment, the sequence of $\dot{\phi}$ points arranged in an order of increasing values, as described before, would then correspond to a sequence of θ values on the circle, where r is the maximum value of $\dot{\phi}$, and θ_0 is a constant. From this relation, we have calculated $\theta - \theta_0$ using the measured values of $\dot{\phi}$ at the peaks for two different winding numbers, each set is arranged in an order of increasing $\dot{\phi}$ (or $\theta - \theta_0$), as shown in Fig. 6.

In order to find d_n for the determination of α, one needs to identify a point corresponding to $\theta=0$ on the cir-

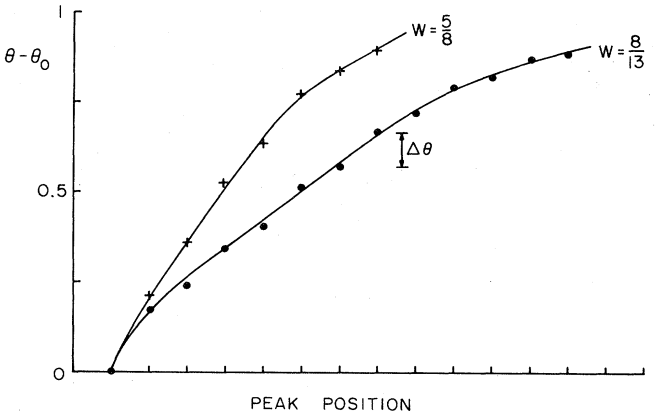

FIG. 6. θ plots derived from the measured peak values of $\dot{\phi}$ and $\dot{\phi}_{\text{peak}} = \dot{\phi}_{\max}\cos(\theta - \theta_0)$; marks on abscissa correspond to peak positions in the $\dot{\phi} - t$ plots (in arbitrary units).

cle. This is difficult from an experimental point of view. Nevertheless, we have applied an approximation that for $|\theta| \ll 1$ in the case of $|K| < 1$ and large n, the circle map $f^{F_n}(\theta)$ reduces to a linear map which can be associated with the region of linear θ variation in Fig. 6. It can be seen from the θ plots in Fig. 6 that a linear region exists in each plot where the change in θ between successive points is more or less constant. Without knowing which of these points exactly corresponds to $\theta=0$, we have taken the average of $\Delta\theta$ which is the increment of θ between two successive points near $\theta=0$ (modulo 1 in the circle map), by using several points in this linear region; this procedure is equivalent to finding a best fit to the slope of the straight-line portion of each θ plot. This average value of $\Delta\theta$ obtained with a winding number $W_n=F_n/F_{n+1}$ is called d_n. For instance, from the θ plots in Fig. 6, we have found $d_6=1.01\pm0.1$, $d_5=1.69\pm0.1$, and computed $\alpha_6=d_5/d_6=1.67\pm0.2$. By using several sets of θ plots, such as in Fig. 6, obtained with different combinations of A_1 and A_2, we have found an average value,

$$\alpha_6=1.63\pm0.2\ . \tag{7}$$

It is interesting to see that although rather crude approximations have been introduced in this procedure, the average value of α obtained with $n=6$ in the sequence of measured $\dot{\phi}$ peak values is in agreement with the circle-map calculation. The sign of α, however, cannot be determined by this method.

IV. CONCLUSION

By using an electronic Josephson-junction simulator, we have carried out physical observations of the quasiperiodic behavior of this system. When driven by two independent ac sources, the system exhibits certain scaling behavior with a special set of rational winding numbers, in reasonable agreement with circle-map calculations. The Poincaré section in the $\sin\phi-\dot{\phi}$ plane with a winding number $W=P/Q$ shows a set of Q stationary points residing on the trajectory of an ellipse when low driving-current amplitudes are applied. These Q discrete points turn into a continuous curve of invariant ellipse when the winding number W is well approximated by an irrational number, namely the reciprocal of the golden mean. This ellipse may be compared with an invariant circle. If the current amplitudes are increased, the system shows a change from quasiperiodicity to chaos similar to a phase transition, characterized by the breakdown of a smooth invariant ellipse (i.e., appearance of kinks at the onset sometimes accompanied by a splitting of the nearly elliptic traces) and a chaotic power spectrum.

These observations lend direct support to the predicted behavior of quasiperiodicity and transition to chaos, which are different from the routes through period-doubling bifurcation and intermittency. Our results may be interpreted either as experimental evidence for these effects associated with an electronic nonlinear circuit, or as analog solutions to the differential equation shown in Eq. (1). Taking the former interpretation, these experimental results may be viewed as providing the first measurement of the two predicted universal constants δ and α pertaining to quasiperiodicity. Although only terms up to $n=6$ in the sequence with $W_n=F_n/F_{n+1}$ have been measured, the experimental values of $\delta=-2.75\pm0.2$ and $|\alpha|=1.63\pm0.2$ are in reasonable agreement with those obtained with a circle map.

On the other hand, if these data are regarded as analog solutions to Eq. (1), our results then indicate that if a Josephson junction or a damped pendulum were driven by two oscillatory sources, a route to chaos following the predictions of a circle map could exist. This route to chaos is also of technical interest in the case of a Josephson junction driven by two ac's, because the situation is similar to that for parametric amplifiers or microwave mixers where the Josephson junction is used as the basic nonlinear element. Our results suggest that if the ratio of two input frequencies happens to lie very close to an irrational number, numerous sidebands could occur, and if the local oscillator amplitude is higher than a critical value, an increase of the chaotic noise level as high as 60 dB or more could appear at the device output.

ACKNOWLEDGMENT

We would like to thank S. Kivelson and J. Sethna for fruitful discussions.

[1]For a recent review see, for example, J.-P. Eckmann, Rev. Mod. Phys. 53, 643 (1981), and references cited therein.

[2]M. J. Feigenbaum, J. Stat. Phys. 19, 25 (1978); 21, 669 (1979); Commun. Math. Phys. 77, 65 (1980).

[3]P. Manneville and Y. Pomeau, Phys. Lett. 75A, 1 (1979); Commun. Math. Phys. 74, 189 (1980).

[4]M. J. Feigenbaum, L. P. Kadanoff, and S. J. Shenker, Physica 5D, 370 (1982); S. J. Shenker, *ibid.* 5D, 405 (1982); D. Rand, S. Ostlund, J. Sethna, and E. D. Siggia, Phys. Rev. Lett. 49, 132 (1982); S. Ostlund, D. Rand, J. Sethna, and E. Siggia (unpublished).

[5]B. A. Huberman, J. P. Crutchfield, and N. H. Packard, Appl. Phys. Lett. 37, 750 (1980); R. L. Kautz, J. Appl. Phys. 52, 6241 (1981); N. F. Pedersen and A. Davidson, Appl. Phys. Lett. 39, 830 (1981); M. R. Beasley and B. A. Huberman, Comments Solid State Phys. (in press); A. H. MacDonald and M. Plischke, Phys. Rev. B 27, 201 (1983); E. Ben-Jacob, I. Goldhirsch, Y. Imry, and S. Fishman, Phys. Rev. Lett. 49, 1599 (1982).

[6]W. J. Yeh and Y. H. Kao, Phys. Rev. Lett. 49, 1888 (1982); Appl. Phys. Lett. 42, 299 (1983).

[7]J. H. Magerlein, Rev. Sci. Instrum. 49, 486 (1978).

[8]W. C. McCumber, J. Appl. Phys. 39, 3113 (1968).

[9]P. Coullet and C. Tresser, Phys. Lett. 77A, 327 (1980).

[10]P. Bak (private communication).

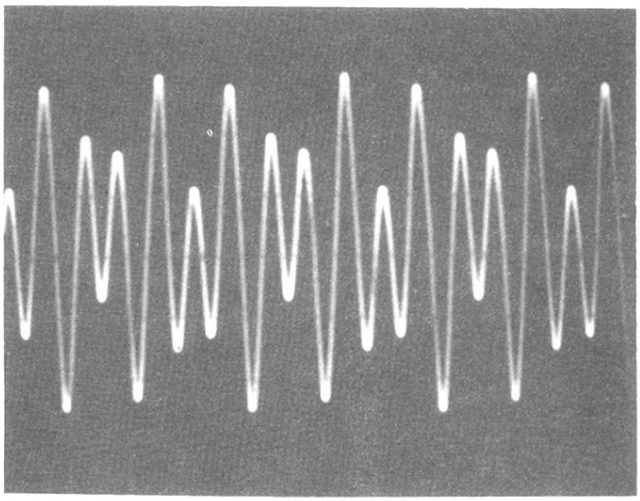

(a)

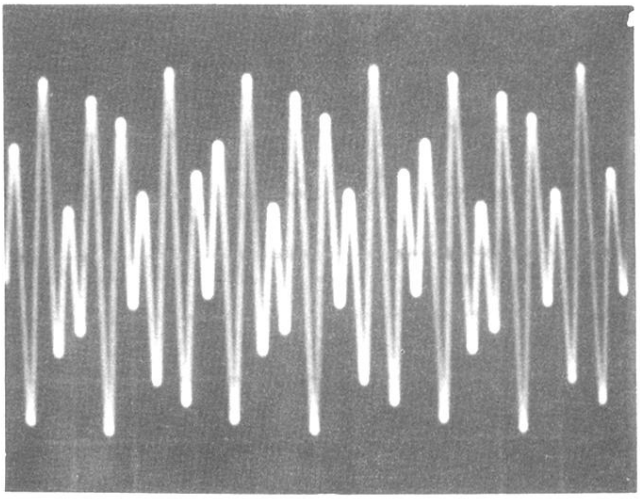

(b)

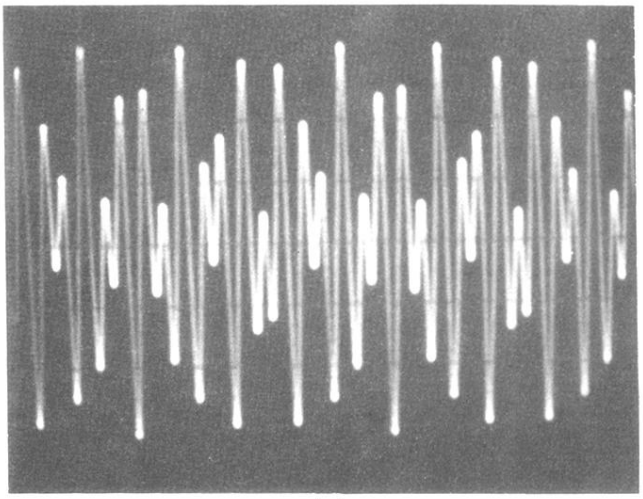

(c)

FIG. 2. Oscilloscope traces of $\dot{\phi}(t)$ vs t. (a) $\omega_1 \cong 0.65$, $\omega_2 = 1.09$, $W = \frac{3}{5}$, $A_1/A_{1c} = 0.192$, and $A_2/A_{2c} = 0.096$. (b) $\omega_1 \cong 0.68$, $\omega_2 = 1.09$, $W = \frac{5}{8}$, $A_1/A_{1c} = 0.143$, and $A_2/A_{2c} = 0.101$. (c) $\omega_1 \cong 0.67$, $\omega_2 = 1.09$, $W = \frac{8}{13}$, $A_1/A_{1c} = 0.252$, and $A_2/A_{2c} = 0.101$.

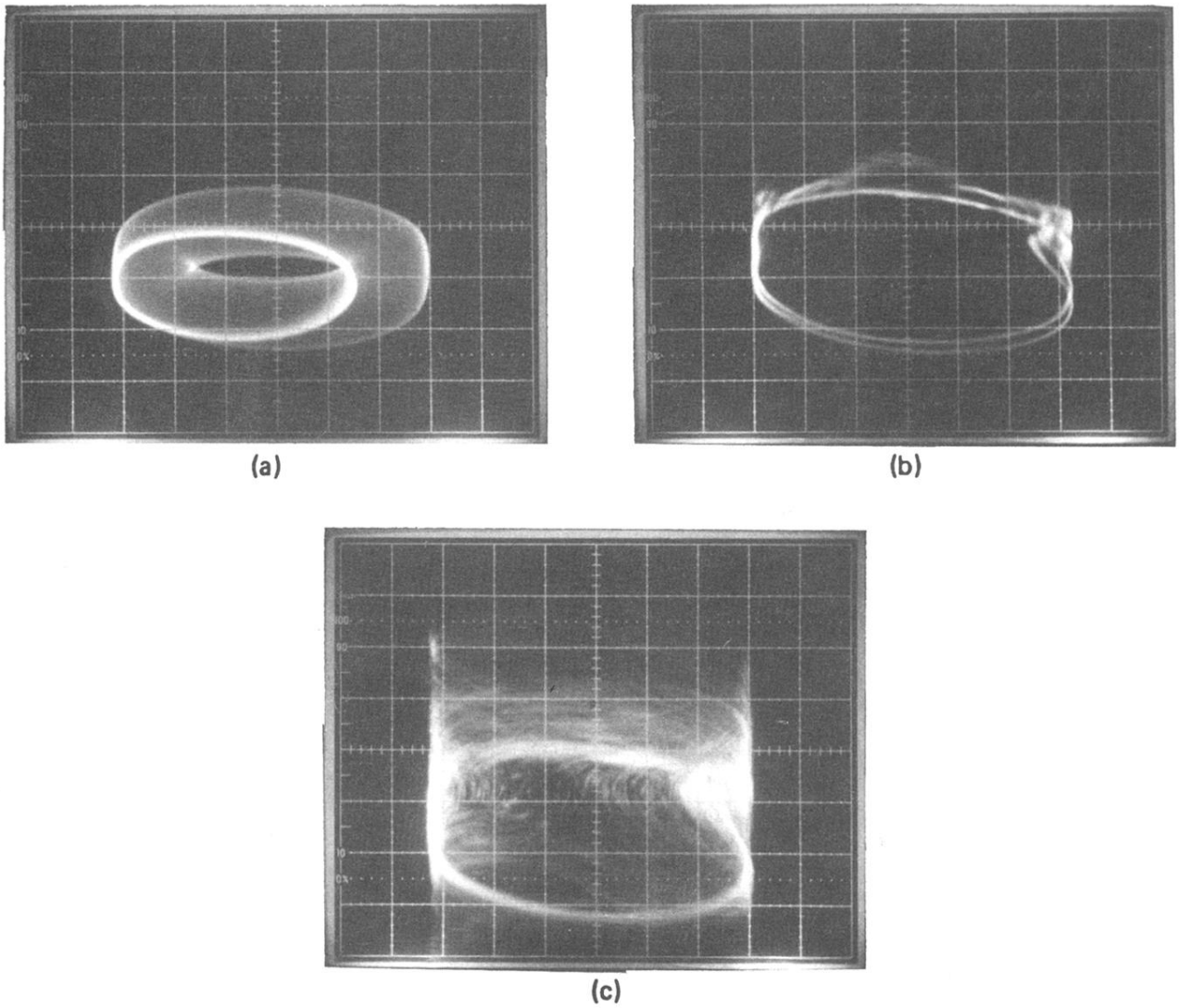

FIG. 3. Sequence of Poincaré sections from quasiperiodicity to chaos obtained by plotting $\sin\phi$ against $\dot{\phi}$; $\omega_1=0.4059$, $\omega_2=0.6568$, $\omega_1/\omega_2\cong\overline{W}$. (a) The bright ellipse is obtained with a discrete time interval (z axis triggering the oscilloscope beam at a frequency equal to that of V_2, 3.0 kHz). $A_1=0.5224$ and $A_2=0.1600$. The torus is the same plot of $\sin\phi$ vs $\dot{\phi}$ with the same parameters except that free running time is used (internal triggering instead of z-axis triggering.) (b) Onset of chaos characterized by the appearance of kinks. $A_1=0.7651$ and $A_2=0.1608$. (c) Chaotic regime. $A_1=0.7656$ and $A_2=0.1608$.